RESEARCH LETTER

Effects of static stress triggering of the strongest earthquakes along the Bengco—southeastern Piedmont of Nyainqentanglha mountain fault zone, Tibet

Gang Yang [ORCID] · Jianchao Wu · Qing Hu · Yongjian Cai

Abstract In this paper, we calculate the Coulomb stress changes triggered by the four strongest earthquakes (M ≥ 6.3) occurred along the Bengco—southeastern piedmont of Nyainqentanglha mountain fault zone in 1411 (M8.0), in 1951 (7.7), in 1952 (M7.4), and 2008 (M6.3). We demonstrate that each strong earthquake occurred in the area where Coulomb stress had been increased (0.018~1.353 bar) by the prior major earthquakes. For example, the Coulomb stress of M7.7 earthquake in 1951 increased by 0.874 bar by the M8.0 earthquake in 1411. The Coulomb stress of M7.4 earthquake in 1952 increased by 1.353 bar by the M7.7 earthquake in 1951. However, the Coulomb stress of M6.3 earthquake in 2008 increased only by 0.018 bar by the M7.4 earthquake in 1952. The 1411, 1951, and 1952 prior strong earthquakes brought cumulative Coulomb stress triggering effects on the Nimu segment of the southeastern piedmont fault of Nyainqentanglha mountain, which is related with the occurrence of the M6.3 earthquake in 2008. The result shows that all of the strong earthquakes on the Bengco—southeastern piedmont of Nyainqentanglha mountain fault zone since 1411 were triggered by a series of prior strong earthquakes and tectonic stress loading.

G. Yang · J. Wu · Q. Hu · Y. Cai
Key Laboratory of Earthquake Geodesy, Institute of Seismology, China Earthquake Administration, Wuhan 430071, China

G. Yang (✉) · J. Wu · Q. Hu · Y. Cai
Wuhan Institute of Earthquake Engineering, Wuhan 430071, China
e-mail: yangg8710@126.com

1 Introduction

Stress triggering refers to the effect of static stress increase on the nearby faults caused by co-seismic dislocations of the prior earthquake, which may trigger new earthquakes minutes or decades after the prior earthquake (Freed 2005). The numerical method is often used to calculate and analyze whether the occurrence of major earthquakes was affected by the triggering of the prior earthquake, and whether the occurrence of large earthquakes will change the stress state on the nearby faults (King et al. 1994; Stein et al. 1997; Zhu and Wen 2010). Studying the spatial pattern and migration rule of earthquakes is an important basis for earthquake prevention and disaster reduction work. The result is also one of the important evidence for plate tectonics research (Zhou et al. 2003).

The Tibetan Plateau experienced a strong uplift since the Late Pleistocene (Fig. 1). The crustal deformation of the central part of the plate is mainly E-W extensional and develops a series of near S-N tectonic belts, including the southeastern piedmont fault of Nyainqentanglha mountain (SPFNM) (Jiao et al. 2015). Four strong earthquakes occurred on the Bengco—southeastern piedmont of Nyainqentanglha mountain (B-SPNM) fault zone, which are the Damxung M8.0 earthquake

in 1411, the Bengco M7.7 earthquake in 1951, the Gulu M7.4 earthquake in 1952, and the Damxung M6.3 earthquake in 2008 (Fig. 1).

Central Tibet is a region of strong seismicity, and it is also a strong tectonic active area. The distribution of the epicenters in the Tibetan Plateau has a good correspondence with the active tectonic zone. The epicenter-concentrated zone mainly distributes on the active faults in the NW, NE, and nearly N-S directions (Wu et al. 1994). East-West sutures (such as the YarlungZangbo suture) have no obvious epicenter dense zones (Wu et al. 1992). The Bengco fault zone was formed before the late Yanshanian movement. The latest activity of the Bengco fault occurred in 1951, which led to the Bengco M7.7 earthquake in 1951 and produced an earthquake surface rupture of 81 km along the fault zone. The SPFNM was formed in Cretaceous and has been active for many times since Late Quaternary. The three recent strong activities of the SPFNM occurred in 1411, 1952, and 2008, which led to the Damxung M8.0 earthquake in 1411, the Gulu M7.4 earthquake in 1952, and the Damxung M6.3 earthquake in 2008, respectively. The latest activity time of the YarlungZangbo fault is Late Pleistocene (Wu et al. 1992; Peng and Wang 2013).

In this paper, the Coulomb stress analysis methods are used to study the stress changes caused by those strong earthquakes in the B-SPNM fault zone.

2 Principles, methods, and calculation procedures

When a strong earthquake occurs, co-seismic dislocations will cause static stress changes on the fault planes in the nearby vicinity. When the Coulomb stress variation on the adjacent fault is positive, the fault will slip again and may increase the probability of following earthquakes soon. This is the stress triggering effect of an earthquake (King et al. 1994). When the change of the Coulomb stress on the adjacent fault is negative, the likelihood of the fault slipping again is reduced. Generally speaking, the positive area of the Coulomb stress changes is the stress trigger area, and the negative area is the stress shadow area (Harris and Simpson 1998). Earthquakes and ruptures that cause stress changes are called source earthquakes and source faults, respectively. Other pre-existing faults in the area are called receiver faults (King et al. 1994; Stein 1999).

For the stress-transfer analysis, this paper adopts the uniform isotropic elastic half-space model proposed by

Okada (1992) and the Coulomb stress variation formula developed by King et al. (1994). The static Coulomb stress change ($\Delta\sigma_f$) caused by strong earthquakes in the fault zone during the period of 1411–2008 was calculated using the Coulomb 3.3 software (Lin and Stein 2004; Toda et al. 2005) according to the Coulomb stress principle

$$\Delta\sigma_f = \Delta\tau_s + \mu'\Delta\sigma_n \qquad (1)$$

where $\Delta\tau_s$ is the shear stress change on a given failure plane (positive in the fault slip direction), $\Delta\sigma_n$ is the normal stress change (positive for fault unclamping or compression), and $\mu' = \mu(1-\beta)$ is the effective coefficient of friction, which includes the effects of pore pressure changes and generally ranges from 0 to 0.8. β is the Skempton's coefficient that ranges from 0 to 1. Lin and Stein (2004) showed that the μ' is typically found to be around 0.4 ($\mu = 0.75$, $\beta = 0.47$) for subduction zones. Previous studies (Stein and Lisowski 1983; Oppenheimer et al. 1988; Larsen et al. 1992) have employed values of $0.2 \leq \mu' \leq 0.75$ to compute the Coulomb stress changes and have discussed the robustness of the obtained results for different settings of the apparent coefficient of friction. In this paper, there are still some uncertainties in the Coulomb stress calculation. The uncertainties come from the setting of the parameters relative to the stratified crust model and to the physical parameters of the fault. We investigated $\mu' = 0.2$, 0.4, 0.6, and 0.8, respectively. Our results showed no significant differences, which is consistent with previous conclusions. A priori, the models with $\mu' = 0.4$ can minimize the uncertainty, as discussed by King et al. (1994). Therefore, we considered the computation results with $\mu' = 0.4$ for the following analysis and discussion. By assuming a Young's modulus of 8.0×10^5 bar and a Poisson's ratio of 0.25, we compute the Coulomb stress change in an elastic half-space. Positive values of the Coulomb stress change ($\Delta\sigma_f$) promote rupture and negative values inhibit rupture. The Coulomb stress increases as above as 0.1 bar can trigger the occurrence of subsequent aftershocks (Reasenberg and Simpson 1992; King et al. 1994). Toda et al. (1998) considered that the stress triggering threshold was 0.2 bar but some authors claim that there is no stress triggering threshold (Ziv and Rubin 2000; Ogata 2005).
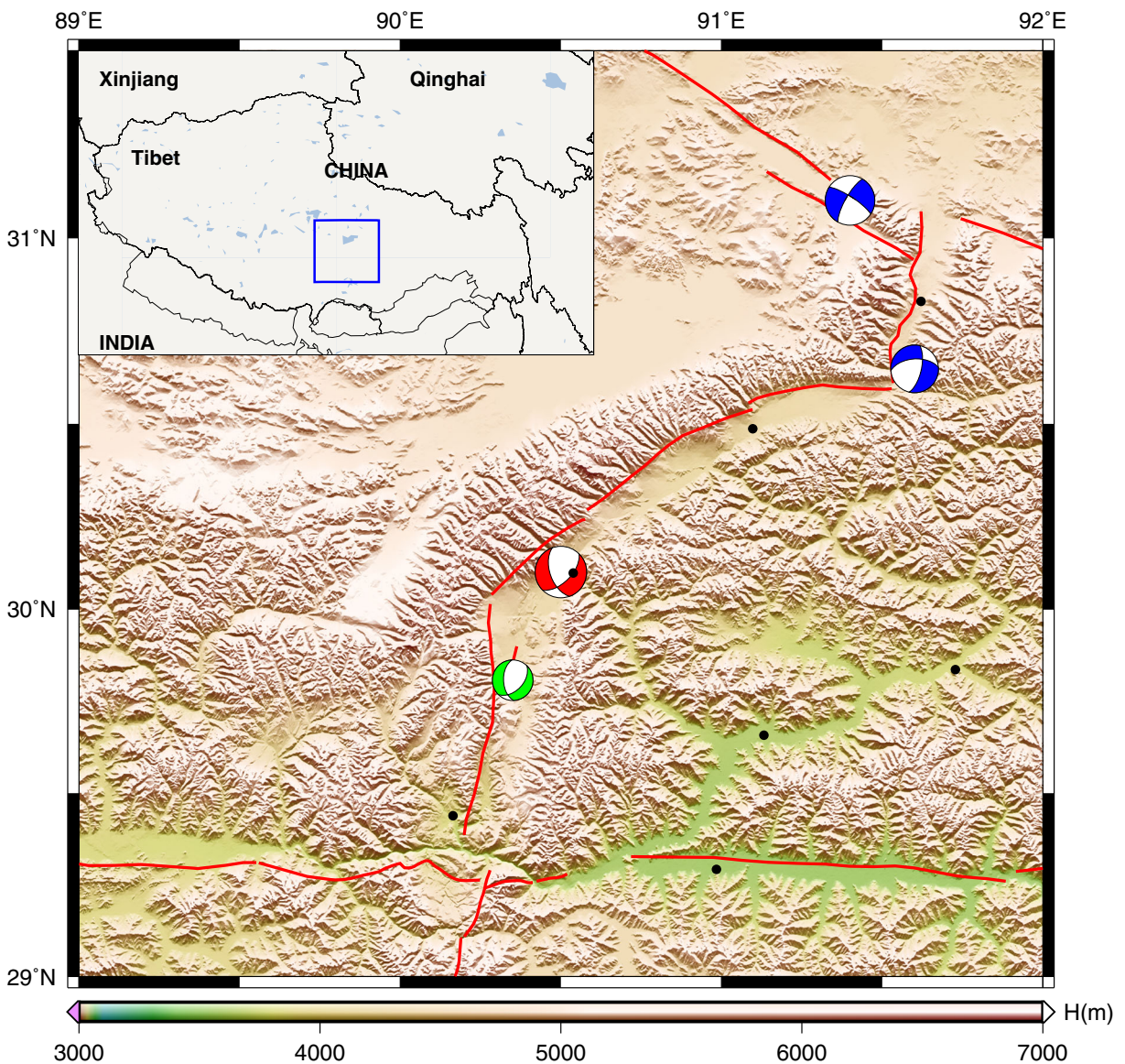
Fig. 1 Seismotectonic map of central Tibet. F1 is the Bengco fault, F2 is the SPFNM—southeastern piedmont fault of Nyainqentanglha mountain (F2-1 Gulu segment, F2-2 Damxung-Yangbajain segment, F2-3 Nimu segment), F3 is the YarlungZangbo fault. DEM data from CGIAR-CSI (2018). The focal mechanisms are the epicenters of the four earthquakes analyzed in this work

3 Seismogenic fault occurrence and co-seismic dislocation model

To compute the Coulomb stress variation, we need to know the characteristic parameters of the source fault and of the receiver fault (strike, dip, rake), and the amount of co-seismic dislocations on the source fault (the co-seismic strike-slip and dip-slip components on the fault plane). For the present earthquakes, the input values can be calculated using seismic fault parameters derived from inversion of seismic wave records, seismic site geological surveys, or geodetic data. For the historical earthquakes, the relevant parameters can only be estimated by empirical methods (Zhu and Wen 2010). According to the existing literature, the strike and dip of the seismogenic fault can be obtained, and then the rake can be calculated based on the horizontal displacement and vertical displacement of the fault. Finally, the Coulomb stress model parameters will be established.

3.1 Damxung M8.0 earthquake in 1411

The source rupture direction of the Damxung M8.0 earthquake in 1411 was 45° (Wu et al. 1992), and its seismogenic fault was the Damxung segment of the southeastern piedmont fault of Nyainqentanglha mountain, and the fault plane tended to Southeast. Therefore, the strike of the seismogenic fault was 45°, the dip was 50°~66° (Wu 2004), and the average value was 58°. According to the vertical and horizontal displacement of the surface rupture (Wu et al. 1992), the average value of rake is estimated to be − 42°.

The results of the earthquake investigations show that the surface rupture length of the seismogenic fault of this earthquake was 108 km (Wu et al. 1992). According to the empirical formulas for the surface rupture length (SRL) and the average co-seismic dislocation (AD) of strike-slip earthquake (Wells and Coppersmith 1994),

$$Log(AD) = -1.70 + 1.04 \times Log(SRL) \qquad (2)$$

$$RS = AD \times TAN(Rake) \qquad (3)$$

Here, SRL is the surface rupture length (km) and AD is the average displacement (m). RS is the reverse slip displacement (m). We estimate that the average right-lateral horizontal slip of the co-seismic dislocation is − 2.60 m. According to the slip angle of the fault plane, the reverse slip of the co-seismic dislocation is estimated to be − 2.34 m. Right-lateral is positive, and reverse slip is positive [m].

3.2 Bengco M7.7 earthquake in 1951

The rupture direction of the seismogenic fault of the Bengco M7.7 earthquake in 1951 was 300°~305°. The average strike of the seismogenic fault was 303°, and the dip of the seismogenic fault was 78° (Wu et al. 1992). The focal depth was 30 km (USGS 2015a). The rake calculated is − 165°. The surface rupture length of the seismogenic fault of this earthquake was 81 km (Wu et al. 1992).

According to formulas (2) and (3), the average right-lateral horizontal slip of the co-seismic dislocation is 1.93 m and the reverse slip of the co-seismic dislocation is − 0.52 m.

3.3 Gulu M7.4 earthquake in 1952

The source rupture direction of the Gulu M7.4 earthquake in 1952 was about 13°, the seismogenic fault was the Gulu segment of the SPFNM, and the fault plane tended to East. Therefore, the strike of the seismogenic fault was 13° (Wu et al. 1992). The average dip of the seismogenic fault was 67° (Liu et al. 2009). The focal depth was 25 km (USGS 2015b). The rake calculated is about − 142°. The surface rupture length of the seismogenic fault of this earthquake was 57.7 km (Wu et al. 1992).

According to formulas (2) and (3), the average right-lateral horizontal slip of the co-seismic dislocation is 1.35 m and the reverse slip of the co-seismic dislocation is estimated to be − 1.06 m.

3.4 Damxung M6.3 earthquake in 2008

The seismogenic fault of the Damxung M6.3 in 2008 earthquake was the Nimu segment of the SPFNM, and the surface rupture length was 20 km (Wu and Ye 2009). The focal depth was 12 km, strike was 44°, dip was 48°, and rake was − 53° (USGS 2014).

According to formulas (2) and (3), the average right-lateral horizontal slip of the co-seismic dislocation is − 0.45 m. According to the slip angle of the fault plane, the reverse slip of the co-seismic dislocation is estimated to be − 0.60 m.

4 Stress evolution and earthquake triggering

According to the parameters listed in Table 1, we calculated the Coulomb stress changes on the fault plane of the four earthquakes caused by the co-seismic dislocation of each earthquake in chronological order (Fig. 2).

Figure 2 a shows that the Bengco M7.7 earthquake in 1951 was located in the area where the co-seismic Coulomb failure stress was significantly increased due to the Damxung M8.0 earthquake in 1411. The Coulomb stress at the center of the rupture increased by 0.874 bar. Figure 2 b shows that the Gulu M7.4 earthquake in 1952 was also located in the area where the co-seismic Coulomb failure stress was significantly increased due to the Bengco M7.7 earthquake in 1951. The Coulomb stress at the center of the rupture increased by 1.353 bar. Figure 2 c shows that the Damxung M6.3 earthquake in 2008 was also located

Table 1 Parameters of the seismogenic faults of M ≥ 6.3 earthquakes in the study area from 1411 to 2008

| No.	Date	Long. lat. (°)	M	Depth (km)	Location	Strike/dip/rake (°)	SRL (km)	Right-lateral (m)	Reverse slip (m)
1	Sep 28, 1411	90.5/30.1	8.0	30.0	Damxung	45/58/− 42	108	− 2.60	− 2.34
2	Nov 18, 1951	91.4/31.1	7.7	30.0	Bengco	303/78/− 165	81	1.93	− 0.52
3	Aug 17, 1952	91.601/30.648	7.4	25.0	Gulu	13/67/− 142	57.7	1.35	− 1.06
4	Oct 6, 2008	90.350/29.807	6.3	12.0	Damxung	44/48/− 55	20	− 0.45	− 0.60

in the area where the co-seismic Coulomb failure stress was slightly increased due to the Gulu M7.4 earthquake in 1952. The Coulomb stress at the center of the rupture increased by 0.018 bar.

Figure 3 a shows that Coulomb stress changes on the fault plane of the Gulu M7.4 earthquake in 1952 caused by the co-seismic dislocations of the Damxung M8.0 earthquake in 1411 and Bengco M7.7 earthquake in 1951. The cumulative Coulomb stress changes at the center of the rupture increased by 1.395 bar. Figure 3 b shows that the Damxung M6.3 earthquake in 2008 was located in the area where the co-seismic Coulomb failure stress was significantly increased due to the Damxung M8.0 earthquake in 1411, Bengco M7.7 earthquake in 1951, and Gulu M7.4 earthquake in 1952. The cumulative Coulomb stress changes at the center of the rupture increased by 0.691 bar.

5 Discussion

Based on the seismic stress triggering theory and elastic dislocation theory, the Coulomb stress changes on the rupture plane was computed according to the focal mechanism solutions of each M ≥ 6.3 earthquake since 1411. The results showed that the strong earthquakes occurred in the loading area of the prior strong earthquakes and the Coulomb stress increase zone. The increase of the Coulomb stress produced by strong earthquakes is beneficial to the occurrence of subsequent earthquakes. The earthquake caused by the increase of the Coulomb stress mostly occurs on the fault plane not far from the previous epicenter.

There are three different seismic trigger stress threshold views: 0.2 bar (Toda et al. 1998), 0.1 bar (Reasenberg and Simpson 1992; King et al. 1994), and no threshold (Ziv and Rubin 2000; Ogata 2005). After
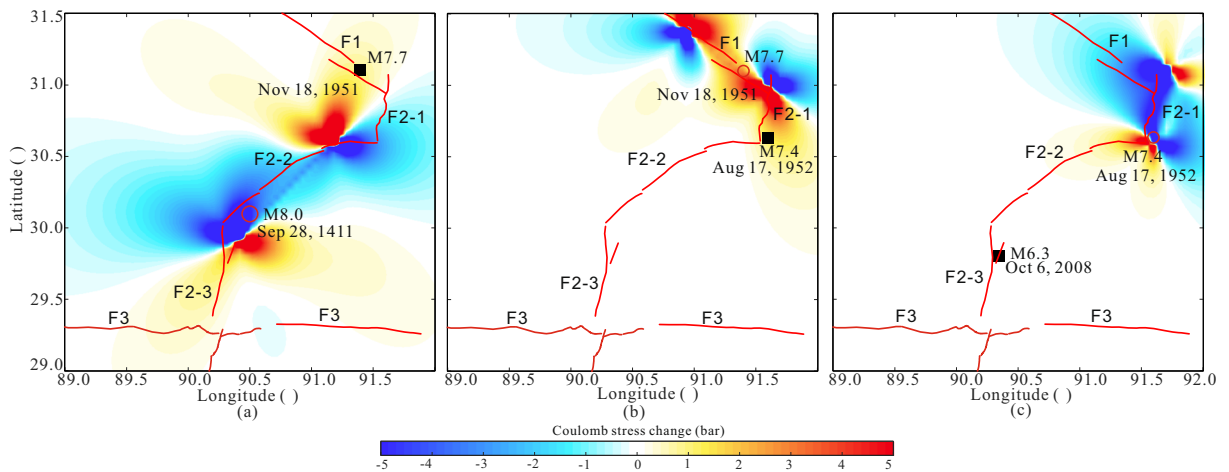
Fig. 2 Coulomb failure stress changes caused by the co-seismic dislocations on the fault zone. **a** Coulomb stress changes on the 1951 M7.7 earthquake's fault plane associated with the co-seismic dislocation of the 1411 M8.0 earthquake; source fault is F2-2, specified receiver fault plane is 303 (strike), 78 (dip), − 165 (rake), and the calculated depth is 30.0 km. **b** Coulomb stress changes on the 1952 M7.4 earthquake's fault plane associated with the co-seismic dislocation of the 1951 M7.7 earthquake; source fault is F1, specified receiver fault plane is 13 (strike), 67 (dip), − 142 (rake), and the calculated depth is 25.0 km. **c** Coulomb stress changes on the 2008 M6.3 earthquake's fault plane associated with the co-seismic dislocation of the 1952 M7.4 earthquake; source fault is F2-1, specified receiver fault plane is 44 (strike), 48(dip), − 55 (rake), and the calculated depth is 12.0 km. Red circle represents source earthquake. The black square represents the epicenter of later earthquake on the receiver fault
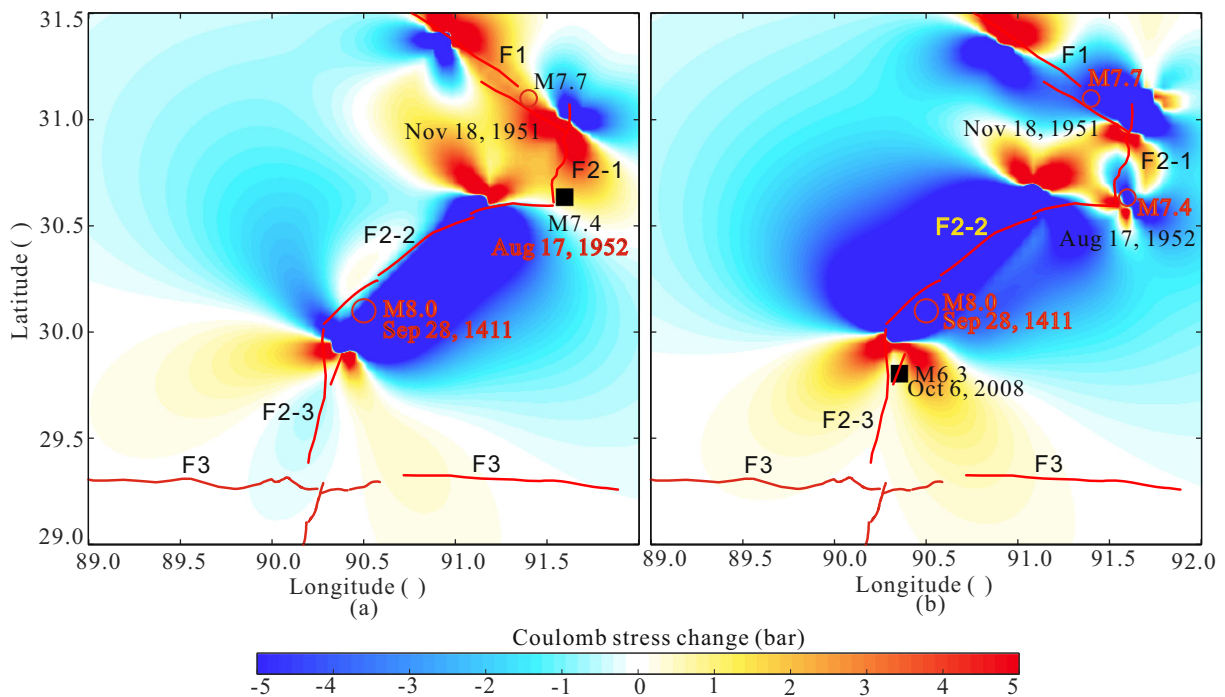
Fig. 3 Cumulative Coulomb failure stress changes caused by the co-seismic dislocations of prior earthquakes on the fault zone since 1411. **a** Coulomb stress changes associated with the co-seismic dislocation of the 1411 M8.0 earthquake and the 1951 M7.7 earthquake; source fault is F2-2, F1, specified receiver fault plane is 13 (strike), 67(dip), − 142 (rake), and the calculated depth is 25.0 km. **b** Coulomb stress changes caused by the co-seismic dislocation of prior earthquakes just before the 2008 M6.3 earthquake; source fault is F2-2, F1, and F2-1, specified receiver fault plane is 44 (strike), 48 (dip), − 55 (rake), and the calculated depth is 12.0 km. Red circle represents source earthquake. The black square represents the epicenter of later earthquake on the receiver fault

an earthquake occurred, it had less Coulomb stress increase value at longer distance. For instance, Fig. 2 c shows that the increase of the Coulomb stress at the center of the Damxung M6.3 earthquake in 2008 was 0.018 bar associated with the co-seismic dislocation of the 1952 event, and the distance between them was 169 km. Whether this earthquake was triggered by the last single earthquake's Coulomb stress change or the prior earthquakes' cumulative Coulomb stress trigger, it is difficult to get an exact conclusion. An earthquake is likely to be related to all prior earthquakes' Coulomb stress accumulation, long-term tectonic loading, and so on. The single triggering effect of earthquake factors has not been proven.

Therefore, we consider that the Damxung M6.3 earthquake in 2008 was triggered by the co-seismic dislocation of prior earthquakes before 2008. Meanwhile, Fig. 3 b shows that the increase of cumulative Coulomb stress changes at the center of the rupture of the Damxung M6.3 earthquake in 2008 was 0.691 bar caused by the co-seismic dislocation of prior

earthquakes before 2008. We were unable to test the triggering threshold, but the triggering threshold should be less than 0.691 bar.

We consider that the cumulative Coulomb stress can explain the triggering effect better than the co-seismic Coulomb stress changes alone for the earthquakes series. This has also been demonstrated in other areas in the world, e.g., California (Verdecchia and Carena 2016) and Italy (Mildon et al. 2017).

In this study, the large earthquake triggered (e.g., Bengco M7.7 earthquake in 1951) by the Coulomb stress change did not occur on the fault segment (F2-1) immediately adjacent to the prior large earthquake (Damxung M8.0 earthquake in 1411) rupture, but occurred after jumping over the fault segment adjacent to the first rupture (F1). However, if the two fault zones (e.g., F1 and F2-1) intersect, the Coulomb stress generated by the prior earthquake (Bengco M7.7 earthquake in 1951) may accumulate in the post-earthquake zone (Gulu M7.4 earthquake in 1952).

Therefore, whether a fault with a significant increase in the Coulomb stress will trigger a strong aftershock, it seems that depending on whether the fault already has a high and near-critical stress accumulation background (Zhu and Wen 2012).

6 Conclusion

Based on the seismic stress triggering theory and the elastic dislocation theory, we compute the Coulomb stress changes induced by the strongest earthquakes ($M \geq 6.3$) occurred on the B-SPNM fault zone from 1411 to 2008 in central Tibet. We analyzed the static stress triggering effects induced by the individual prior earthquakes to the next strong earthquake. Main conclusions of this study are derived:

(1) Between 1411 and 2008, each earthquake ($M \geq 6.3$) occurred in the area where the Coulomb stress had been increased by the prior earthquake(s).
(2) After an earthquake occurred, it had less Coulomb stress increase value at a longer distance.
(3) Whether a fault with a significant increase in the Coulomb stress will trigger a strong earthquake, it depends whether the fault already has a high and near-critical stress accumulation background.

References

CGIAR-CSI (2018) http://srtm.csi.cgiar.org/srtmdata/

Freed AM (2005) Earthquake triggering by static, dynamic, and post seismic stress transfer. Annu Rev Earth Planet Sci 33: 335–367. https://doi.org/10.1146/annurev.earth.33.092203.122505

Harris RA, Simpson RW (1998) Suppression of large earthquakes by stress shadows: a comparison of Coulomb and rate-and-state failure. J Geophys Res 103(B10):24439. https://doi.org/10.1029/98JB00793

Jiao QS, Zhang JF, Jiang WL (2015) Geomorphic features and remote sensing research of fault activity along the southeastern piedmont faults of Nyenchen Tonglha Mountains. Dizhen Dizhi 37(2):613–626. https://doi.org/10.3969/j.issn.0253-4967.2015.02.022 (in Chinese with English abstract)

King GCP, Stein RS, Lin J (1994) Static stress changes and the triggering of earthquakes. Bull.seism.soc.am 84(3):935–953

Larsen S, Reilinger R, Neugebauer H, Strange W (1992) Global positioning system measurements of deformations associated with the 1987 Superstition Hills earthquake: evidence for conjugate faulting. J Geophys Res Solid Earth 97(B4):4885–4902. https://doi.org/10.1029/92JB00128

Lin J, Stein RS (2004) Stress triggering in thrust and subduction earthquakes and stress interaction between the southern San Andreas and nearby thrust and strike-slip faults. J Geophys Res Solid Earth 109(B2). https://doi.org/10.1029/2003JB002607

Liu J, Shen XH, Meng K, Chen ZW, Dai YQ, Xu YR, Jing F, Hong SY (2009) Preliminary studies on the Late Quaternary activity of the western margin fault of Gulu Basin. Tibet Earthquake 29(3):45–53 in Chinese with English abstract

Mildon ZK, Roberts GP, Faure Walker JP, Iezzi F (2017) Coulomb stress transfer and fault interaction over millennia on non-planar active normal faults: the Mw 6.5-5.0 seismic sequence of 2016-2017, central Italy. Geophys J Int 210(2):1206–1218. https://doi.org/10.1093/gji/ggx213

Ogata Y (2005) Detection of anomalous seismicity as a stress change sensor. J Geophys Res Solid Earth 110(5):1–14. https://doi.org/10.1029/2004JB003245

Okada Y (1992) Internal deformation due to shear and tensile faults in a half-space. Bull Seismol Soc Am 82(2):1018–1040

Oppenheimer DH, Reasenberg PA, Simpson RW (1988) Fault plane solutions for the 1984 Morgan Hill, California, earthquake sequence: evidence for the state of stress on the Calaveras fault. J Geophys Res Solid Earth 93(B8):9007–9026. https://doi.org/10.1029/JB093iB08p09007

Peng XL, Wang DY (2013) Structural characteristics and activity analysis of the YarlungZangbo fault zone. J Yangtze Univ (Nat Sci Edit) 10(26):41–44 (in Chinese with English abstract)

Reasenberg PA, Simpson RW (1992) Response of regional seismicity to the static stress change produced by the Loma Prieta earthquake. Science 255(5052):1687–1690. https://doi.org/10.1126/science.255.5052.1687

Stein RS (1999) The role of stress transfer in earthquake occurrence. Translated World Seismol 402(6762):605–609. https://doi.org/10.1038/45144

Stein RS, Lisowski M (1983) The 1979 Homestead Valley earthquake sequence, California: control of aftershocks and postseismic deformation. J Geophys Res Solid Earth 88(B8):6477–6490. https://doi.org/10.1029/JB088iB08p06477

Stein RS, Barka AA, Dieterich JH (1997) Progressive failure on the North Anatolian fault since 1939 by earthquake stress triggering. Geophys J Int 128(3):594–604. https://doi.org/10.1111/j.1365-246X.1997.tb05321.x

Toda S, Stein RS, Reasenberg PA, Dieterich JH, Yoshida A (1998) Stress transferred by the 1995 Mw=6.9 Kobe, Japan, shock: effects on aftershocks and future earthquake probabilities. J Geophys Res 103(b10):24543–24565. https://doi.org/10.1029/98jb00765

Toda S, Stein RS, Richards-Dinger K, Bozkurt SB (2005) Forecasting the evolution of seismicity in southern California: animations built on earthquake stress transfer. J Geophys Res 110(B5):B05S16. https://doi.org/10.1029/2004JB003415

USGS (2014) M6.3 - eastern Xizang. https://earthquake.usgs.gov/earthquakes/eventpage/usp000gjgt#executive

USGS (2015a) M 7.7 - eastern Xizang. https://earthquake.usgs.gov/earthquakes/eventpage/iscgem894960/origin/detail

USGS (2015b) M 7.4 - eastern Xizang. https://earthquake.usgs.gov/earthquakes/eventpage/iscgem893286#executive

Verdecchia A, Carena S (2016) Coulomb stress evolution in a diffuse plate boundary: 1400 years of earthquakes in eastern California and western Nevada, USA. Tectonics. 35(8): 1793–1811. https://doi.org/10.1002/2015TC004091

Wells DL, Coppersmith KJ (1994) New empirical relationships among magnitude, rupture length, rupture width, rupture area, and surface displacement. Bull Seismol Soc Am 84(4):974–1002

Wu ZH (2004) Quaternary geology and active faults in the Damxung-Yangbajain basin and adjacent area, central Tibet. Chinese Academy of Geolgecal Sciences, Beijing (in Chinese with English abstract)

Wu ZH, Ye PS (2009) The seismic intensity, seismogenic tectonics and mechanism of the Ms6.6 Damxung earthquake happened on October 6, 2008 in southern Tibet, China. Geological Bulletin of China 28(6):713–725 (in Chinese with English abstract)

Wu ZM, Cao ZQ, Shen-tu BM, Deng QD (1992) Active faults in the central Tibet. Seismological Press, Beijing (in Chinese with English abstract)

Wu ZM, Cao ZQ, Shen-tu BM, Deng QD (1994) Seismogenic tectonics in the central Tibet. Earthquake Research China 10(1):19–27 in Chinese with English abstract

Zhou CH, Pei T, Li QL, Chen JB, Wang ZS (2003) Research on spatial pattern and temporal-spatial migration model of strong earthquakes in China and its adjacent areas. Earth Sci J China Univ Geosci 28(3):306–314 in Chinese with English abstract

Zhu H, Wen XZ (2010) Static stress triggering effects related with Ms8.0 Wenchuan earthquake. J Earth Sci 21(1):32–41. https://doi.org/10.1007/s12583-010-0001-8

Zhu H, Wen XZ (2012) Effects of static stress triggering of the major earthquake sequence on Xiaojiang-Zemuhe fault zone. Earth Sci J China Univ Geosci 37(1):199–206 (in Chinese with English abstract)

Ziv A, Rubin AM (2000) Static stress transfer and earthquake triggering: no lower threshold in sight? J Geophys Res 105(B6):13631–13642. https://doi.org/10.1029/2000JB900081